

${}^3\text{He}(e,e'p)d$ and ${}^3\text{He}(e,e'p)pn$ at high momentum transfer

Results from the Jefferson Lab E89-044 experiment

D.W. Higinbotham, for the Jefferson Lab Hall A Collaboration

Jefferson Lab, Newport News, VA 23606 USA

Received: 4 Sep 2003 / Accepted: 14 Nov 2003 /

Published Online: 6 Feb 2004 – © Società Italiana di Fisica / Springer-Verlag 2004

Abstract. The $(e,e'p)$ reaction has proven to be a useful tool for studying specific aspects of the nucleus. The Jefferson Lab continuous electron beam accelerator facility (CEBAF) along with the high resolution spectrometers in the Hall A end station allow this reaction to be studied in kinematics heretofore inaccessible. In this paper the results of the Jefferson Lab Hall A ${}^3\text{He}(e,e'p)d$ and ${}^3\text{He}(e,e'p)pn$ measurements, performed at a fixed $\mathbf{q}=1.5$ GeV/c and $\omega=840$ MeV, will be presented along with theoretical calculations by G. Salme, J.-M. Laget, and J. Udias.

PACS. 21.45.+v few-body systems – 25.70.Bc quasielastic scattering

1 Introduction

The E89-044 proposal [1] to study the ${}^3\text{He}(e,e'p)$ reaction at high momentum transfer was one of the original Jefferson Lab Hall A experiments and drove much of the design of the hall and its two high resolution spectrometers. The 2×10^{-4} momentum resolution of these spectrometers allows to separate the ${}^3\text{He}(e,e'p)$ two-body break-up channel from the continuum, a gap of only 2.2 MeV, at incident beam energies in excess of 4800 MeV.

The E89-044 experiment took data over a broad range of kinematics to study the single-nucleon structure of nuclei and to study the behavior of nucleons embedded in the nuclear medium. In this paper, preliminary results from the constant $\mathbf{q}=1.5$ GeV/c and $\omega=840$ MeV portion of the experiment for both the ${}^3\text{He}(e,e'p)d$ and ${}^3\text{He}(e,e'p)pn$ reactions will be presented along with theory calculations by G. Salme, J.-M. Laget, and J. Udias. New calculations by C. Ciofi degli Atti are presented elsewhere in these proceedings.

2 Kinematics

The kinematics for the $(e,e'p)$ reaction are shown in Fig. 1. The scattering plane is defined by the incoming electron, $e = (E_e, \mathbf{e})$, and the outgoing electron, $e' = (E'_e, \mathbf{e}')$. The four-momentum of the virtual photon is given by $q^\mu = (\omega, \mathbf{q})$ and the four-momentum of the outgoing proton is given by $p'^\mu = (E_p, \mathbf{p}')$. The four-momentum square, $Q^2 = q^2 - \omega^2$, is defined such that for electron scattering Q^2 is always positive. The missing momentum vector is defined as $\mathbf{p}_m = \mathbf{q} - \mathbf{p}'$ and represents the momentum of the recoiling system.

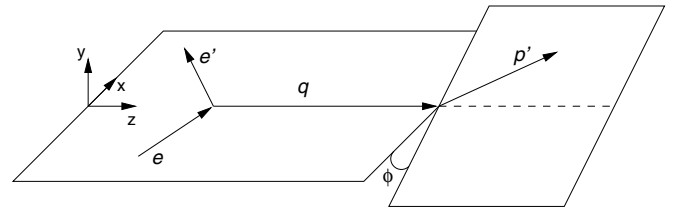


Fig. 1. A schematic of the kinematics for the $(e,e'p)$ reaction

The form of the differential cross section for $(e,e'p)$ reactions in the one-photon exchange approximation without polarization is:

$$\frac{d^6\sigma}{d\Omega_{e'} dE_{e'} d\Omega_{p'} dE_{p'}} = \frac{E_p p'}{(2\pi)^3} \sigma_{Mott} [v_T R_T + v_L R_L + v_{TL} R_{TL} \cos \phi + v_{TT} R_{TT} \cos 2\phi], \quad (1)$$

with ϕ the angle between the plane defined by \mathbf{e} and \mathbf{e}' and the plane defined by \mathbf{p}' and \mathbf{q} , and σ_{Mott} the Mott cross section,

$$\sigma_{Mott} = \frac{4\alpha^2 E_e^2}{Q^4} \cos^2 \frac{\theta_e}{2}. \quad (2)$$

The kinematical factors v_L, v_T, v_{TL} , and v_{TT} are:

$$v_L = \frac{Q^4}{q^4}, \quad (3)$$

$$v_T = \frac{Q^2}{2q^2} + \tan^2(\theta_e/2), \quad (4)$$

$$v_{TL} = \frac{Q^2}{q^2} \left[\frac{Q^2}{q^2} + \tan^2(\theta_e/2) \right]^{1/2}, \text{ and} \quad (5)$$

$$v_{TT} = \frac{Q^2}{2q^2}. \quad (6)$$

For the two-body break-up channel, ${}^3\text{He}(e,e'p)d$, the proton energy and angle with respect to \mathbf{q} are correlated because the missing energy is fixed. In this case the differential cross is written as

$$\frac{d^5\sigma}{d\Omega_{e'}d\Omega_{p'}dE_{e'}} = \frac{E_{p'}}{(2\pi)^3} \sigma_{Mott} f_{rec}^{-1} [v_T R_T + v_L R_L + v_{TL} R_{TL} \cos \phi + v_{TT} R_{TT} \cos 2\phi], \quad (7)$$

where f_{rec} is the recoil factor,

$$f_{rec} = \left[1 - \frac{E_{p'} \mathbf{p}_m \cdot \mathbf{p}'}{E_t p'^2} \right]. \quad (8)$$

The response functions, R_L, R_T, R_{TL}, R_{TT} can be separated by a suitable choice of the kinematic parameters. In perpendicular in-plane kinematics at a fixed \mathbf{q} and ω , one can separate R_T, R_{TL} , and a combination of the R_L and R_{TT} response functions, denoted as R_{L+TT} . One can also measure the cross-section asymmetry A_{TL} for a given \mathbf{q} and ω . This asymmetry is defined as:

$$A_{TL} = \frac{\sigma(\phi = 180^\circ) - \sigma(\phi = 0^\circ)}{\sigma(\phi = 180^\circ) + \sigma(\phi = 0^\circ)}. \quad (9)$$

3 Theory

The cross-section results presented in this paper will be compared with a plane-wave impulse approximation (PWIA) calculation by Salme *et al.* [2] and the microscopic calculations of J.-M. Laget. The A_{TL} asymmetry will be compared with a relativistic mean-field calculation by J.M. Udias along with Laget's microscopic calculation. The details of the microscopic and relativistic calculations are presented below.

3.1 Microscopic calculation

In the microscopic calculation performed by J.-M. Laget, the reaction amplitude is expanded in diagrams which are computed in momentum space [3]. The code used the Urbana V14 potential and relativistic kinematics. For the PWIA calculation, the possibility of the virtual photon coupling to either the initial state proton or the deuteron is taken into account. In the full calculations of J.-M. Laget, two-body and three-body mechanisms such as final-state interactions and meson-exchange currents are taken into account.

3.2 Relativistic mean-field calculation

In the relativistic mean-field calculations performed by J.M. Udias [5], the one-body nucleon current is calculated with relativistic wave functions for the initial bound and

final outgoing nucleons. The bound-state wave function is represented by a four-spinor. The spinors in a completely relativistic calculation are often referred to as *distorted* because of the presence of the scalar and vector potentials appearing in the lower component [6,7]. The spinor is obtained by solving the Dirac equation with scalar-vector potentials. Proton distortions are calculated solving the Dirac equation using an optical potential. The Jefferson Lab Hall A ${}^{16}\text{O}(e,e'p){}^{15}\text{N}$ response function and A_{TL} asymmetry results [8] were well described by this type of calculation [9,10]. While a mean-field calculation cannot reproduce the ${}^3\text{He}(e,e'p)$ cross section, it will be shown that it does describe the general characteristics of the extracted A_{TL} asymmetry.

4 Results

4.1 Two-body break-up

In order to isolate the two-body break-up channel from the continuum, the $(e,e'p)$ data was plotted as a function of missing energy. Due to the high momentum resolution of the Hall A spectrometers, even with a 4.8 GeV electron beam it was possible to fit the two-body peak and separate it from the continuum which, as a function of missing energy, begins only 2.2 MeV from the two-body peak. The MCEEP code [11] was used to calculate acceptance and to take radiative corrections into account.

In Figs. 2, 3, and 4 the results of the ${}^3\text{He}(e,e'p)d$ cross-section extractions are shown. These results are all for a fixed $\mathbf{q} = 1.5 \text{ GeV}/c$ and $\omega = 840 \text{ MeV}$, but were taken at different values of ϕ and ϵ to allow response-function separations. The cross-section in Fig. 2 is for $\phi = 180^\circ$ and $\epsilon = 0.94$ and in Fig. 3 is for $\phi = 0^\circ$ and $\epsilon = 0.94$. Combining these results using 7 the R_{TL} response function can be extracted and by using 9 the A_{TL} asymmetry, as shown in Fig. 5, can be extracted. The cross section results shown in Fig. 4 are for $\phi = 180^\circ$ and ϵ of 0.11. Combining this result with those shown in Fig. 2 will allow the R_T and R_{L+TT} response functions to be extracted.

These results can be divided into three distinct ranges in missing-momentum. The first is the low missing momentum range from 0 to 200 MeV/c where the PWIA models describe the data reasonably well. The second region from 200 to 700 MeV/c requires the inclusion of final-state interactions and meson-exchange currents to reproduce the enhancement in the cross sections and cause oscillations in the A_{TL} asymmetry. The third region, around 1000 MeV/c, presently cannot be explained by any model. The forthcoming response function separations will further test the models and allow a deeper understanding of the reaction mechanisms.

4.2 Continuum

For the ${}^3\text{He}(e,e'p)pn$ data, the focus was to study the effect of two-nucleon correlations. Previous continuum data

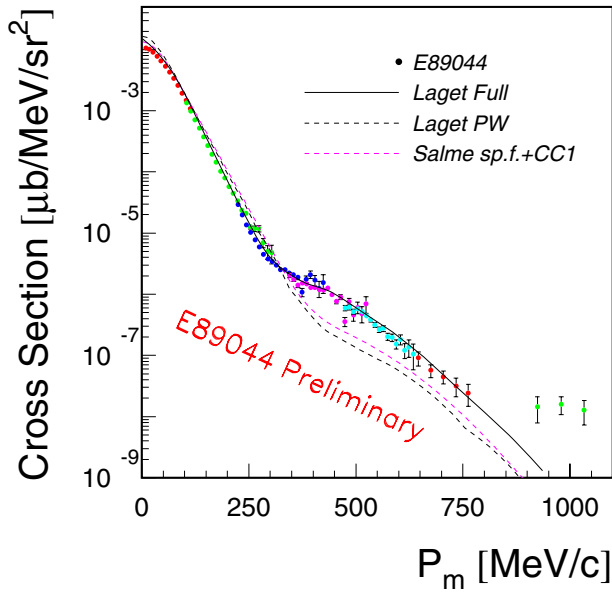


Fig. 2. Shown are the preliminary cross section results for the reaction ${}^3\text{He}(e,e'p)d$ as a function of missing momentum with a beam energy of 4807 MeV and with a fixed $\mathbf{q} = 1500$ MeV/c and $\omega = 840$ MeV [1]. The theory curves show a PWIA calculation along with the latest full calculation of J.M. Laget. The enhancement in the cross section near 300 MeV/c and continuing to larger missing momentum is predominately due to final-state interactions. There is no clear indication yet from theory what causes the enhancement of the cross section near 1000 MeV/c

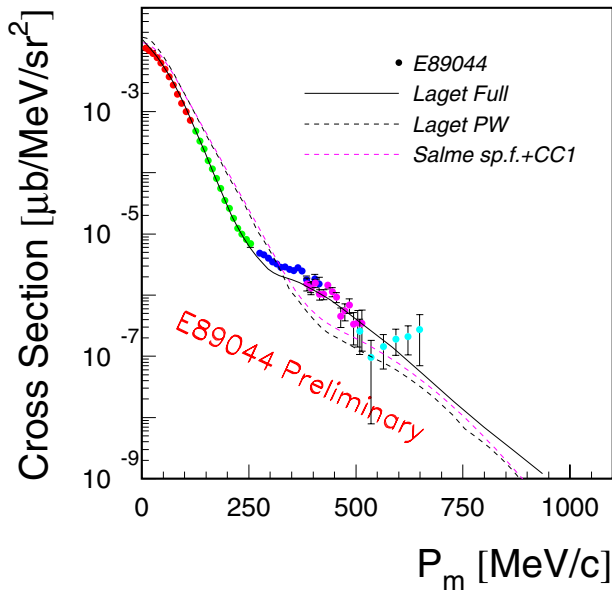


Fig. 3. Shown are the preliminary cross-section results for the reaction ${}^3\text{He}(e,e'p)d$ as a function of missing momentum at a beam energy of 4807 MeV and with a fixed $\mathbf{q} = 1500$ MeV/c and $\omega = 840$ MeV [1]. The theory curves show a PWIA calculation along with the latest full calculation of J.M. Laget

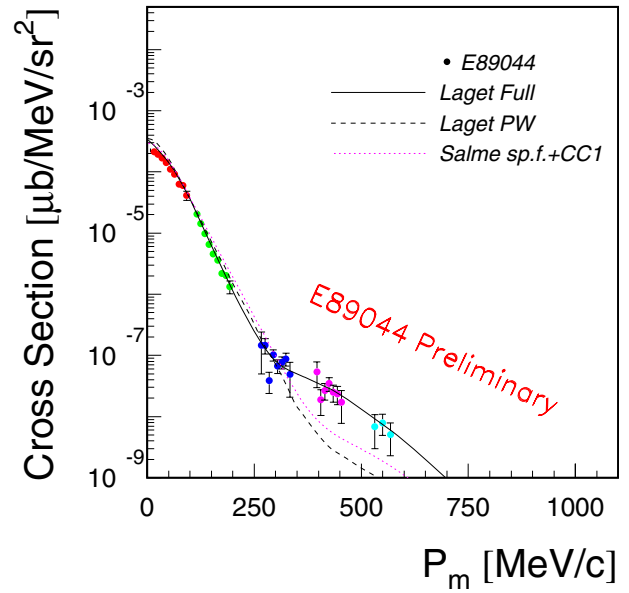


Fig. 4. Shown are the preliminary cross-section results for the reaction ${}^3\text{He}(e,e'p)d$ as a function of missing momentum at a beam energy of 1250 MeV and a fixed $\mathbf{q} = 1500$ MeV/c and $\omega = 840$ MeV [1]. The theory curves show a PWIA calculation along with the latest full calculation of J.M. Laget

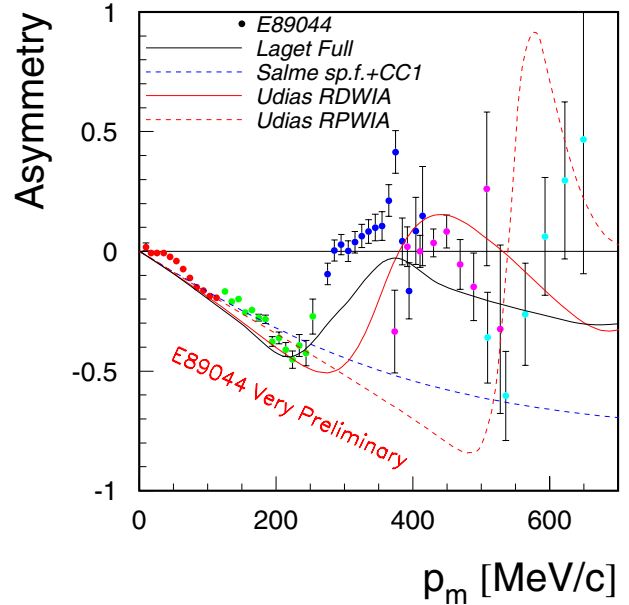


Fig. 5. Shown are the preliminary A_{TL} data. The curves show the latest calculation of J.M. Laget along with a preliminary result of J. Udias. At lower missing momentum the theories are most sensitive to relativistic effects, while at the larger missing momentum the theories become sensitive to final-state interaction effects

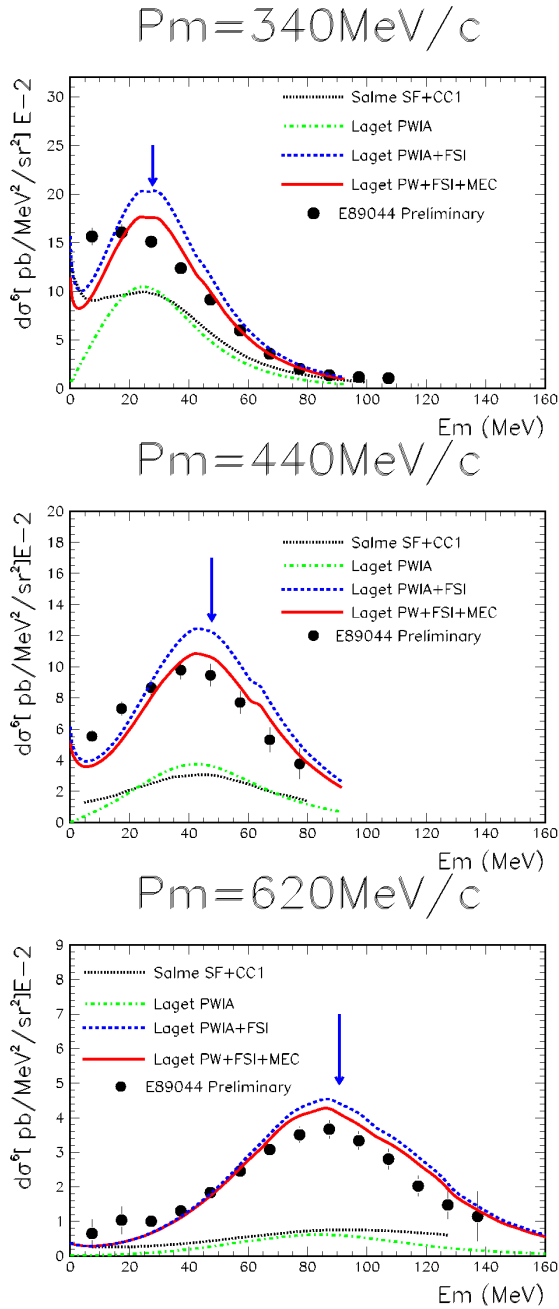


Fig. 6. Shown are the cross-section data for the ${}^3\text{He}(e,e'p)pn$ reaction at a fixed \mathbf{q} and ω as a function of missing energy. The dotted curves show a PWIA prediction of Salme, while the other curves show the theoretical predictions of J.-M. Laget from PWIA to full calculations including meson-exchange current and final-state interaction effects. The arrow shows where one would expect the peak in the cross section due to the photon coupling to a correlated pair of nucleons

on ${}^4\text{He}$ have shown a correlation peak which shifts outward in missing energy as a function of missing momentum as:

$$E_m = E_{thr} + \frac{A-2}{A-1} \times \frac{\mathbf{p}_m^2}{2M_p} \quad (10)$$

where E_{thr} is the missing energy corresponding to the continuum threshold [12]. While these data indicated correlations, they were of limited statistics and response function separations were not made.

Preliminary high statistics Jefferson Lab ${}^3\text{He}(e,e'p)pn$ data are shown in Fig. 6. These results are for a constant $\mathbf{q} = 1.5 \text{ GeV}/c$ and $\omega = 840 \text{ MeV}$, an $\epsilon = 0.94$, and $\phi = 180^\circ$. The peak in the cross-section data in Fig. 6 follows 10 as is indicated by the arrows; though unlike the data of Le Goff *et al.* [12], the cross section appears dominated by final-state interactions. Analysis of the rest of the constant \mathbf{q} and ω continuum data is underway and response functions will be forthcoming.

5 Conclusions

Preliminary results of the constant $\mathbf{q} = 1.5 \text{ GeV}$ and $\omega = 840 \text{ MeV}/c$ part of the Jefferson Lab E89-044 experiment have been presented. As predicted by theory, the cross section is strongly enhanced by final-state interactions for missing momenta greater than 200 MeV/c. At the highest missing momenta, around 1000 MeV/c, the results have yet to be explained by theory.

I would like to acknowledge the hard work and dedication of the doctoral students working on the analysis of the E89-044 experiment: Marat Rvachev with M.I.T., Emilie Penel-Nottaris with Grenoble, and Fatiha Benmokhtar with Rutgers. Also, I would also like to thank the experiment spokespersons, Marty Epstein, Arun Saha, and Eric Voutier, for their hard work and dedication along with the Hall A collaboration and the E89-044 collaboration. This work was supported by DOE Contract No. DE-AC05-84-ER40150 under which the Southeastern Universities Research Association (SURA) operates the Thomas Jefferson National Accelerator Facility.

References

1. M.B. Epstein, A. Saha, and E. Voutier: spokespersons, Selected Studies of the ${}^3\text{He}$ Nuclei through Electrodisintegration at High Momentum Transfer, Jefferson Lab E89-044
2. A. Kievsky, E. Pace, G. Salme, and M. Viviani: Phys. Rev. C **56**, 64 (1997)
3. J.M. Laget: Phys. Rev. D **579**, 333 (1994)
4. J.M. Laget: Phys. Lett. B **199**, 493 (1987)
5. J. Udias: private communication
6. J.M. Udias, J.A. Caballero, E. Moya de Guerra, J.R. Vignote, and A. Escuderos: Phys. Rev. C **64**, 024614 (2001)
7. J.J. Kelly: Phys. Rev. C **60**, 044609 (1999)
8. J. Gao et al.: Phys. Rev. Lett. **84**, 3265 (2000)
9. J.M. Udias et al.: Phys. Rev. C **51**, 3246 (1995)
10. J.M. Udias, J.A. Caballero, E. Moya de Guerra, J.E. Amaro, and T.W. Donnelly: Phys. Rev. Lett. **83**, 5451 (1999)
11. P. Ulmer, MCEEP: Monte Carlo for electro-nuclear coincidence experiments, CEBAF-TN-91-101
12. J.M. Le Goff et al.: Phys. Rev. C **50**, 2278 (1994)